

**NASA TECHNICAL
MEMORANDUM**



NASA TM X-2968

NASA TM X-2968

**EFFECTS OF FLANGES ON PRESSURE
DISTRIBUTION ON A FLAT PLATE
AND ON A CORRUGATED SURFACE
AT MACH NUMBERS FROM 0.60 TO 1.97**

by Albert L. Johns and Merle L. Jones

Lewis Research Center

Cleveland, Ohio 44135

1. Report No. NASA TM X-2968		2. Government Accession No.		3. Recipient's Catalog No.	
4. Title and Subtitle EFFECTS OF FLANGES ON PRESSURE DISTRIBUTION ON A FLAT PLATE AND ON A CORRUGATED SURFACE AT MACH NUMBERS FROM 0.60 TO 1.97				5. Report Date MARCH 1974	
				6. Performing Organization Code	
7. Author(s) by Albert L. Johns and Merle L. Jones				8. Performing Organization Report No. E-7519	
				10. Work Unit No. 501-24	
9. Performing Organization Name and Address Lewis Research Center National Aeronautics and Space Administration Cleveland, Ohio 44135				11. Contract or Grant No.	
				13. Type of Report and Period Covered Technical Memorandum	
12. Sponsoring Agency Name and Address National Aeronautics and Space Administration Washington, D. C. 20546				14. Sponsoring Agency Code	
15. Supplementary Notes					
16. Abstract <p>An experimental investigation was conducted in the Lewis Research Center 8- by 6-Foot Supersonic Wind Tunnel to obtain the static-pressure distribution on a plate in the region of a flange placed normal to the airstream. Tests were conducted on both a flat-plate surface and a corrugated surface using flange heights ranging from 10 to 125 percent of the boundary-layer height. Data were obtained at a zero degree-angle-of-attack and at Mach numbers from 0.60 to 1.97.</p>					
17. Key Words (Suggested by Author(s)) Turbulent boundary layer Flat plate Corrugated skin Boundary layer				18. Distribution Statement Unclassified - unlimited	
19. Security Classif. (of this report) Unclassified		20. Security Classif. (of this page) Unclassified		21. No. of Pages 32	
				22. Price* \$3.00	

CONTENTS

	Page
SUMMARY	1
INTRODUCTION	2
SYMBOLS	2
APPARATUS AND PROCEDURE	3
INSTRUMENTATION	3
CONFIGURATIONS	4
RESULTS AND DISCUSSION	4
SUMMARY OF RESULTS	6
REFERENCES	7

EFFECTS OF FLANGES ON PRESSURE DISTRIBUTION ON A FLAT PLATE AND ON A CORRUGATED SURFACE AT MACH NUMBERS FROM 0.60 TO 1.97

by Albert L. Johns and Merle L. Jones

Lewis Research Center

SUMMARY

An experimental investigation was conducted in the Lewis Research Center 8- by 6-Foot Supersonic Wind Tunnel to obtain the static-pressure field on a flat plate in the region of a flange. The tests were conducted on both a flat-plate surface and a corrugated surface using flange heights ranging from 10 to 125 percent of the boundary-layer thickness. The corrugated surface was tested to provide design data for the Centaur Standard Shroud, which is used on the Titan/Centaur launch vehicle. The shroud has a corrugated surface and two field joint rings (or flanges) that extend beyond the corrugation into the airstream.

Data were obtained at zero degree angle-of-attack only; Mach numbers were varied from 0.60 to 1.97. The plate was flush mounted to the tunnel sidewall with coinciding centerlines.

Boundary-layer data were obtained on the flat plate without corrugations or a flange. The boundary-layer thickness varied from 15.24 centimeters (6.00 in.), maximum at Mach 0.80, to approximately 10.15 centimeters (4.00 in.), minimum at Mach 1.97.

Upstream of the flange the pressure level of the corrugated configuration with a flange height of 2.921 centimeters (1.15 in.) from the plate (1.397 cm (0.55 in.) from the corrugation crest) was approximately the same as the pressure level on the flat plate with a 1.524 centimeters (0.60 in.) flange at both subsonic and supersonic speeds.

For a given flange height, as measured from the plate surface, the addition of corrugations to the plate had the effect of reducing the pressure level upstream of the flange. The effect on the downstream side was a reduced pressure drop. The addition of corrugations also had the effect of shortening the distance over which the pressures were perturbed by the presence of the flange, both upstream and downstream of the flange.

There were little differences in pressure between the corrugation crest and trough, with the exception of the pressure in the immediate vicinity of the flange.

In most instances, from Mach 0.60 to 1.10 the initial peak pressure ahead of a flange on a flat plate occurred at a distance approximately equal to the flange height.

INTRODUCTION

The separation of a turbulent boundary layer in the region of an obstacle such as a field joint ring (or flange) is a phenomenon of technical importance in the design of space launch vehicles. It is necessary for the designer to evaluate this separation phenomenon in terms of its effect on the steady-state pressure distribution on the vehicle surface. The designer must also know the extent of the region over which this phenomenon acts.

References 1 to 4 describe some of the research that has been conducted in the area of flow separation with surface projections partially or fully immersed in a turbulent boundary layer. However, published research of surface projections totally immersed in a turbulent boundary layer at subsonic and supersonic Mach numbers has been rather limited. This report documents the investigation of the effects of flow separation, which is created in subsonic and supersonic turbulent boundary layers by a flange totally or partially immersed in the boundary layer. The specific problem studied is the steady-state pressure field produced by the separation of a turbulent boundary layer upstream and downstream of a flange located on a flat plate with and without corrugated skin. The flange heights varied from 1.524 to 12.70 centimeters (0.60 to 5.00 in.) without corrugations and from 1.524 to 2.921 centimeters (0.60 to 1.15 in.) with corrugation. (Height is measured from plate surface.)

The test was conducted in the Lewis 8- by 6-Foot Supersonic Wind Tunnel over a range of Mach numbers from 0.60 to 1.97. The flat plate was flush mounted to the tunnel sidewall with coinciding centerlines.

SYMBOLS

C_p	pressure coefficient, $(p_1 - P_0)/q_0$
h	flange height, measured from the plate surface
M_0	free-stream Mach number
P_0	free-stream static pressure
p_1	local static pressure
q_0	free-stream dynamic pressure
V_1	local velocity
V_0	free-stream velocity
y	normal distance from plate surface

- δ boundary-layer thickness, height of the boundary layer where local velocity becomes 99 percent of free-stream velocity
- δ^* displacement thickness, a measure of deficiency in mass flow through boundary layer as result of stream having been slowed by friction
- θ momentum thickness, thickness of free-stream flow necessary to make up deficiency in momentum flux within boundary layer

APPARATUS AND PROCEDURE

Figure 1 shows the plate installation in the wind tunnel. The plate was flush mounted to the tunnel side wall with its centerline coinciding with the centerline of the side wall. The plate was located in the modified test section so as to maintain a boundary-layer height greater than 10.16 centimeters (4.00 in.) over most of the Mach number range. The plate containing a boundary layer rake is shown in figure 2(a). The plate was 243.84 centimeters (96.00 in.) long and 121.92 centimeters (48.00 in.) wide with a 15° ramp leading edge. The plate had a thickness of 1.27 centimeter (0.50 in.). A boundary-layer rake with 16 probes (fig. 2(a)) was located 151.61 centimeters (59.69 in.) from the plate leading edge and 2.54 centimeters (1.00 in.) off the plate centerline. The 2.54 centimeters (1.00 in.) offset from the plate centerline was necessary in order to route the rake instrumentation through the plate. Figures 2(b) and (c) show the details of the flat plate and corrugated configuration. The leading-edges of the corrugation were slanted at an angle of 15° and capped. There was a 0.508-centimeter (0.20-in.) gap between the flange and corrugated sections. Figure 2(d) shows the details of a typical corrugated section.

INSTRUMENTATION

The boundary-layer rake had 19 probes. Only the lower 16 probes were used (fig. 3(a)). These 16 probes covered a distance of 20.320 centimeters (8.00 in.) from the plate. The table in figure 3(a) shows the normal distance from the plate to each probe.

The boundary-layer rake was used to survey the local flow field and to measure the boundary-layer height. The rake was located 151.61 centimeters (59.69 in.) from the leading edge of the plate. The flanges were also located at this station on the succeeding tests.

The plate instrumentation is shown in figure 3(b). Thirty-three static-pressure taps were located upstream of the flange, and 22 downstream. This instrumentation was

routed through a slot located on the underside of the plate. The tables in figure 3(b) show the axial location of the plate instrumentation both upstream and downstream of the flange.

The instrumentation layout for the corrugated configurations is shown in figure 3(c). Static-pressure orifices were located along the crest and in the trough corner. With the exception of the corrugation axial station of ± 0.889 centimeter (± 0.35 in.), the static-pressure orifices were located at the same axial location as those on the plate.

Only the 2.921-centimeter (1.15-in.) flange was instrumented (see fig. 3(d)). Three static-pressure taps were located on the flange along the centerline of the plate as follows: (1) Upstream side of flange (face), 0.711 centimeter (0.28 in.) from the flange top; (2) top of flange (top), 0.508 centimeter (0.20 in.) from the aft side of flange; and (3) downstream side of flange (aft), 0.711 centimeter (0.28 in.) from the flange top.

CONFIGURATIONS

A configuration summary is given in table I. Seven configurations were tested: the flat plate with boundary-layer rake, the flat plate with flanges ranging from 1.524 to 12.700 centimeters (0.60 to 5.00 in.) high, and the corrugated skin with flanges 1.524 and 2.921 centimeters (0.60 and 1.15 in.) high. All flanges used were 1.575 centimeters (0.62 in.) wide. The corrugated skin simulated the actual configuration of the launch vehicle shroud, which has two 2.2921-centimeter (1.15 in.) high field splice rings (flanges), measured from the surface on which the corrugations are mounted. In addition, the shroud has some wind screens which are flush with the tops of the corrugations.

RESULTS AND DISCUSSION

The pressure coefficient was computed based on a value of free-stream static pressure p_0 upstream of the plate. In previous calibrations of this tunnel (refs. 5 and 6) a relation was determined among operational variables (compressor speed, flexible nozzle position, second throat position, and plenum chamber suction pressure) such that the flow was most uniform over the length of the test section and so that model pressure distributions most nearly matched those of flight vehicles. Blocking part of the perforated wall with the plate may have affected this calibration slightly, but no attempt was made to account for it. Also, the boundary-layer transition was natural. The average Reynolds number profile for the data presented is shown in figure 4.

A comparison of typical pressure coefficient distribution is shown in figure 5 for the corrugated configuration with 2.921-centimeter flange (the flange extends 1.397 cm above the corrugations) and the flat plate with a 1.524-centimeter flange. The corrugated con-

figuration tends to produce about the same pressure profile ahead of the flange as the flat-plate configuration at both subsonic and supersonic conditions. On the downstream side of the flange, at subsonic Mach numbers, the corrugated configuration has the effect of extending the region over which the expansion and recompression take place. A lower minimum pressure occurs with the flat plate, but beyond that point the corrugated configuration creates a lower pressure throughout the region of pressure recovery.

Figure 6 shows typical examples of the effect of flange height on pressure coefficient for the flat-plate configurations. The data presented are for Mach 0.60 only, but the same trend was observed for the Mach number range from 0.60 to 1.10. Data are presented in a later figure (fig. 12) showing the pressure coefficient against distance from the leading and trailing edges of the flange for each Mach number tested. The pressure coefficient along the plate (for flange heights greater than 1.524 cm) reaches a peak then dips and subsequently rises sharply at the flange face. The first peak occurs at a distance ahead of the flanges approximately equal to the flange height. The minimum pressure on the downstream side generally occurs from about two to four flange heights from the aft side of the flange.

The boundary-layer velocity profiles obtained with the flat plate are shown in figure 7 over the Mach number range tested. The velocity profile was used to obtain the boundary-layer thickness, which is defined as the height where the local velocity becomes 99 percent of the free-stream velocity.

The dimensionless boundary-layer profiles are shown in figure 8. The boundary-layer thickness, displacement thickness, and momentum thickness are presented in figure 9 for the Mach number range tested.

A comparison of the pressure distributions for a flat plate with a boundary-layer rake and a flat plate and a corrugated configuration with a flange height of 1.524 centimeter is shown in figure 10. The flat plate with the 1.524 centimeter flange had a large pressure rise on the compression side (relative to the flat plate with no flange) and a low pressure region on the expansion side of the flange. When the corrugated skin was added to the flat plate, a substantial reduction occurred (relative to the flat plate with flange) in both pressure rise and pressure drop and in the extent of the affected region. This effect of the corrugated configuration prevailed throughout the Mach range tested.

Figure 11 compares the pressure distribution for the flat plate and corrugated configurations with a 2.921-centimeter flange. The results from these configurations showed an effect similar to that of the 1.524-centimeter flange, which is shown in figure 10. However, the difference in magnitude of the pressure level between the flat plate and the corrugated configuration was smaller with the 2.921-centimeter flange than with that of the 1.524-centimeter flange.

The flat plate configuration (fig. 11) with a 2.921-centimeter flange shows an affect of the flange up to 100 centimeters ahead of the flange. The initial peak pressure occurs

approximately 3 centimeters ahead of the flange. The peak values increased with Mach number to $M_0 = 1.20$ and decreased thereafter. Concurrently, the pressure region affected by the flange decreased from 100 centimeters at $M_0 = 0.60$ to about 16 centimeters at $M_0 = 1.97$. On the upstream side of the flange, the corrugated configuration caused both a reduction in the peak pressure level and the region over which the pressure rise occurred. However, the minimum pressure downstream of the flange was about the same for both the flat plate (with flange) and the corrugated configuration through the subsonic range. But at the supersonic conditions the corrugated configuration produced a lower pressure drop (higher local pressure) than the flat plate. The region affected by the expansion-recompression (downstream side of the plate) was smaller with corrugation over the Mach number range.

Three static-pressure orifices were located on the 2.921-centimeter flange along the centerline of the plate. Pressure coefficients for these orifices are given in table II for the Mach number range tested.

Effects of flange height on the pressure coefficient distribution are shown in figure 12 for the flat plate configurations. The pressure coefficient upstream of the flange first peaked at a distance approximately equal to the configuration flange height from $M_0 = 0.60$ to 1.10. The minimum pressure on the downstream side of the plate generally occurred from about two to four flange heights.

SUMMARY OF RESULTS

An experimental investigation was conducted in the Lewis Research Center 8- by 6-Foot Supersonic Wind Tunnel to obtain the static-pressure field on a plate in the region of a flange placed normal to the airstream. Tests were conducted on both a flat plate surface and a corrugated surface using a range of flange heights. The corrugated surface was tested in order to provide design data for the Centaur standard shroud, which is used on the Titan/Centaur launch vehicle. The shroud has a corrugated surface and two field joint rings (or flanges). These extend beyond the corrugation into the airstream. The flat plate was flush mounted to the tunnel sidewall such that the centerlines coincided. Data were obtained at a zero degree angle-of-attack and at Mach numbers from 0.60 to 1.97. The following observations were made:

1. Data from the flat plate, 1.524-centimeter flange configuration and the corrugated plate 2.921-centimeter flange (1.397 cm above the top of the corrugation) configuration indicate that within a range of flange heights, the corrugated sheet acts as a flat plate. The portion of the flange that extends above the corrugations creates essentially the same pressure profile as a flange that extends the same distance above a flat plate. This is particularly true upstream of the flange at all Mach numbers tested and downstream of the flange at supersonic Mach numbers.

2. A flange normal to the flow on a flat plate caused a pressure rise upstream of the flange and a low-pressure region on the downstream side. In general, from Mach 0.60 to 1.10 a pressure peak occurred at a distance equal to the flange height. The minimum pressure on the downstream side of the flange generally occurred about two to four flange heights from the aft side of the flange.

3. The effect of corrugations was to reduce both the magnitude of the pressure change and the length of the regions that were influenced by the flange.

4. In general, there were little differences in the pressures between the corrugation trough and crest, with the exception of the pressures in the immediate vicinity of the flange.

Lewis Research Center,
National Aeronautics and Space Administration,
Cleveland, Ohio, August 8, 1973,
501-24.

REFERENCES

1. Johnson, David F.; and Mitchell, Glenn A.: Experimental Investigation of Two Methods for Generating an Artificially Thickened Boundary Layer. NASA TM X-2238, 1971.
2. Zukoski, Edward E.: Turbulent Boundary-Layer Separation in Front of a Forward-Facing Step. AIAA J., vol. 5, no. 10, Oct. 1967, pp. 1746-1753.
3. Kelly, Thomas C.: A Transonic Investigation of Base Pressures Associated with Shallow Three-Dimensional Rearward-Facing Steps. NASA TN D-2927, 1965.
4. Gran, Robert L.: Step Induced Separation of a Turbulent Boundary Layer. Part I: Experiments in Supersonic Flow. Ph.D. Thesis, California Inst. Tech., 1970.
5. Mitchell, Glenn A.: Blockage Effects of Cone-Cylinder Bodies on Perforated Wind Tunnel Wall Interference. NASA TM X-1655, 1968.
6. Mitchell, Glenn A.: Effect of Model Forebody Shape on Perforated Tunnel Wall Interference. NASA TM X-1656, 1968.

TABLE II. - 2,921-CENTIMETER FLANGE PRESSURE COEFFICIENTS

(a) Flat plate configuration

(b) Corrugated configuration

TABLE I. - CONFIGURATION SUMMARY

Skin	Flange height, cm
Flat plate	a_0
	1.524
	2.921
	6.350
	12.700
Corrugated	1.524
	2.921

^aBoundary layer survey rake.

Mach number	Pressure coefficient, C_p		
	Face	Top	Aft
0.60	0.354	-0.371	-0.332
.80	.452	.394	.348
.90	.483	.416	.368
.95	.487	.450	.403
.978	.484	.481	.431
1.00	.518	.534	.477
1.10	.508	.594	.529
1.20	.532	.588	.480
1.40	.496	.434	.377
1.60	.458	.248	.310
1.80	.402	.158	.265
1.97	.393	.085	.211

Mach number	Pressure coefficient, C_p		
	Face	Top	Aft
0.60	0.297	-0.411	-0.345
.80	.366	.422	.369
.90	.366	.445	.386
.95	.365	.465	.409
.978	.389	.487	.424
1.00	.392	.519	.468
1.10	.409	.536	.476
1.20	.419	.489	.420
1.40	.404	.355	.331
1.60	.363	.176	.278
1.80	.314	.117	.232
1.97	.317	.045	.184

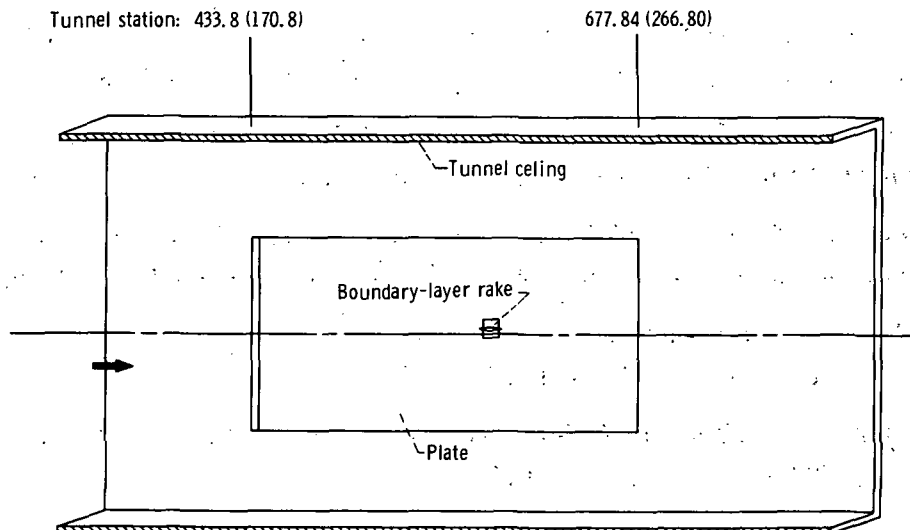
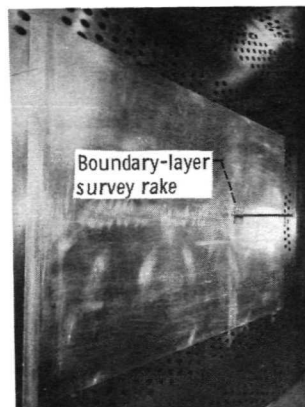
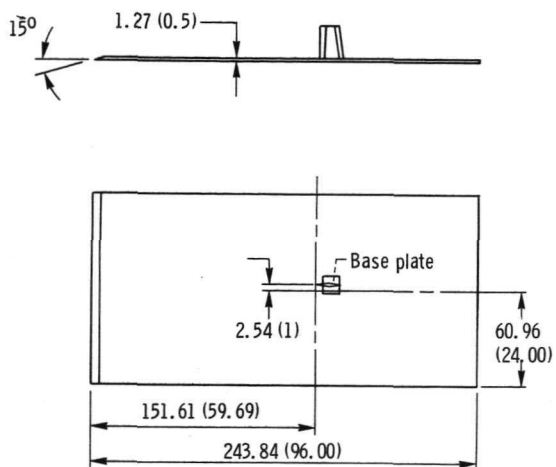
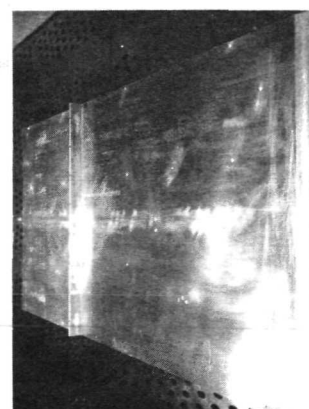
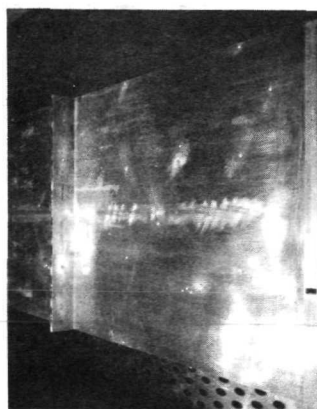
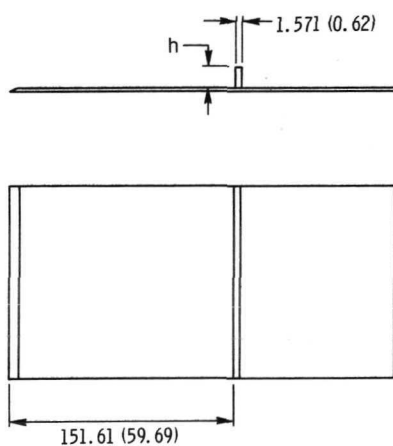
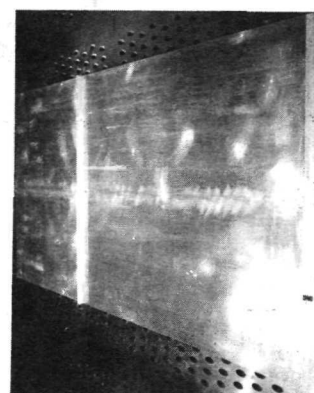
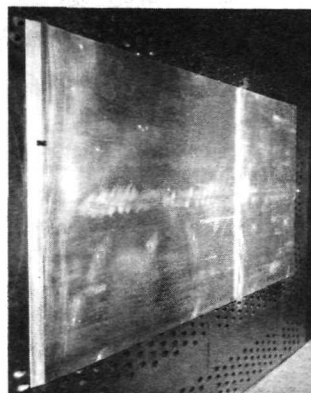


Figure 1. - Plate installation in 8- by 6-foot supersonic wind tunnel. (All dimensions are in cm (in.)).



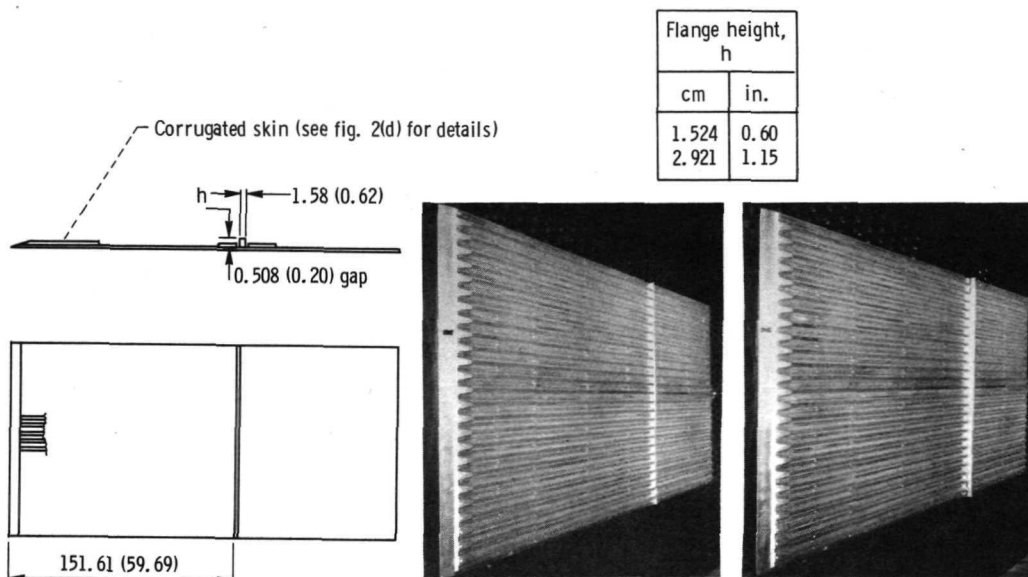
(a) Plate with boundary-layer survey rake.

Flange height, h	
cm	in.
0	0
1.524	.60
2.921	1.15
6.350	2.50
12.700	5.00

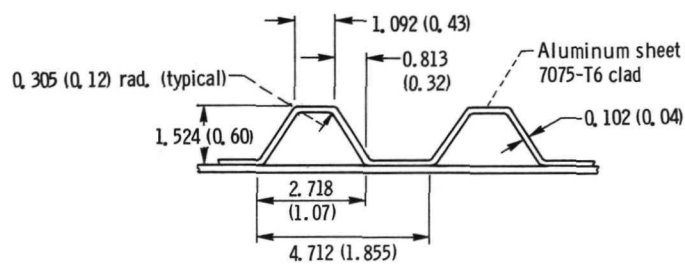


(b) Plate with flange.

Figure 2. - Details of test configurations. (Dimensions are in cm (in.).)



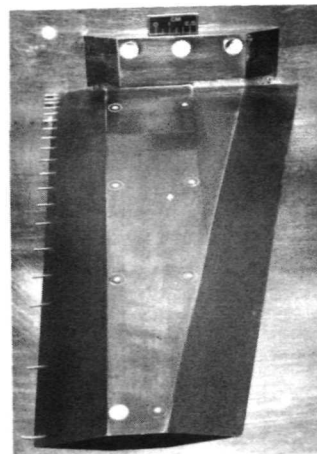
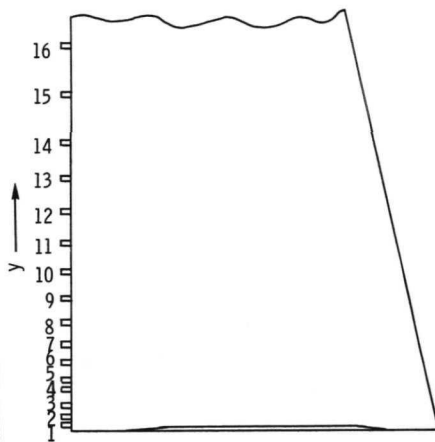
(c) Plate with corrugated skin and flange.



(d) Typical corrugation section.

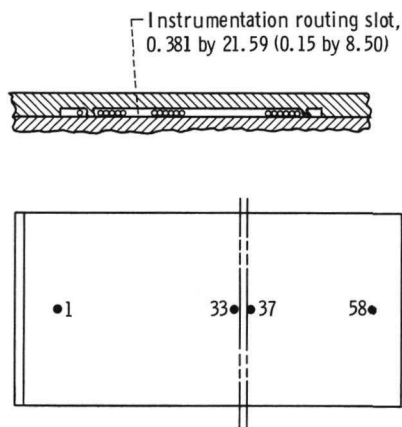
Figure 2. - Concluded.

Probe	y	
	cm	in.
1	0.254	0.10
2	.762	.30
3	1.270	.50
4	1.905	.75
5	2.667	1.05
6	3.556	1.40
7	4.572	1.80
8	5.715	2.25
9	6.985	2.75
10	8.382	3.30
11	9.906	3.90
12	11.557	4.55
13	13.335	5.25
14	15.240	6.00
15	17.780	7.00
16	20.320	8.00



(a) Boundary-layer survey rake.

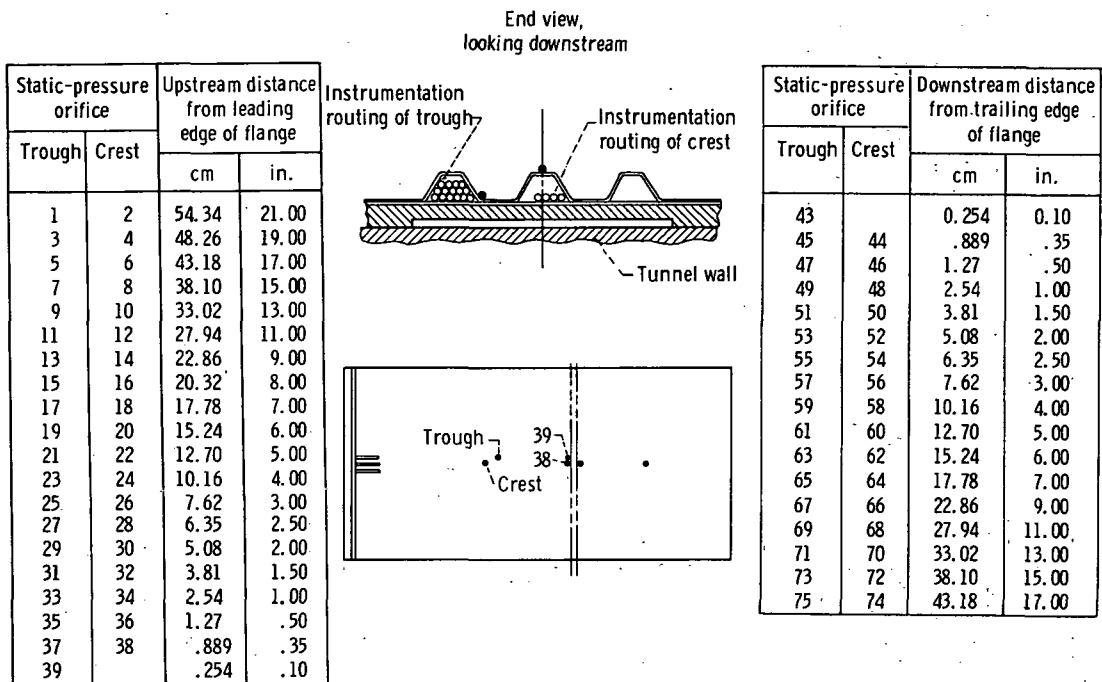
Static pressure orifice	Upstream distance from leading edge of flange	
	cm	in.
1	124.460	49.00
2	119.380	47.00
3	114.30	45.00
4	109.22	43.00
5	104.14	41.00
6	99.06	39.00
7	93.98	37.00
8	88.90	35.00
9	83.82	33.00
10	78.74	31.00
11	73.66	29.00
12	68.58	27.00
13	63.50	25.00
14	58.42	23.00
15	53.34	21.00
16	48.26	19.00
17	43.18	17.00
18	38.10	15.00
19	33.02	13.00
20	27.94	11.00
21	22.86	9.00
22	20.32	8.00
23	17.78	7.00
24	15.24	6.00
25	12.70	5.00
26	10.16	4.00
27	7.62	3.00
28	6.35	2.50
29	5.08	2.00
30	3.81	1.50
31	2.54	1.00
32	1.27	.50
33	.254	.10



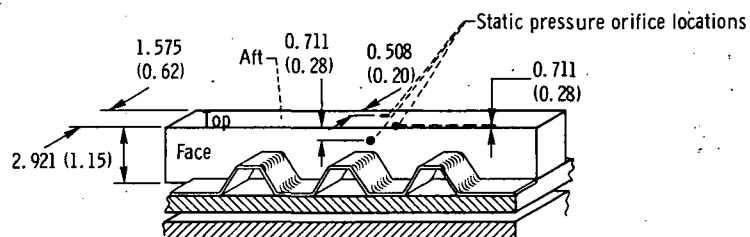
Static pressure orifice	Downstream distance from trailing edge of flange	
	cm	in.
37	0.254	0.10
38	1.27	.50
39	2.54	1.00
40	3.81	1.50
41	5.08	2.00
42	6.35	2.50
43	7.62	3.00
44	10.16	4.00
45	12.70	5.00
46	15.24	6.00
47	17.78	7.00
48	22.86	9.00
49	27.94	11.00
50	33.02	13.00
51	38.10	15.00
52	43.18	17.00
53	48.26	19.00
54	53.34	21.00
55	58.42	23.00
56	63.50	25.00
57	68.58	27.00
58	73.66	29.00

(b) Plate instrumentation.

Figure 3. - Instrumentation. (Dimensions are in centimeters (in.))



(c) Corrugated skin instrumentation.



(d) 2.92-Centimeter (1.15-in.) flange instrumentation.

Figure 3. - Concluded.

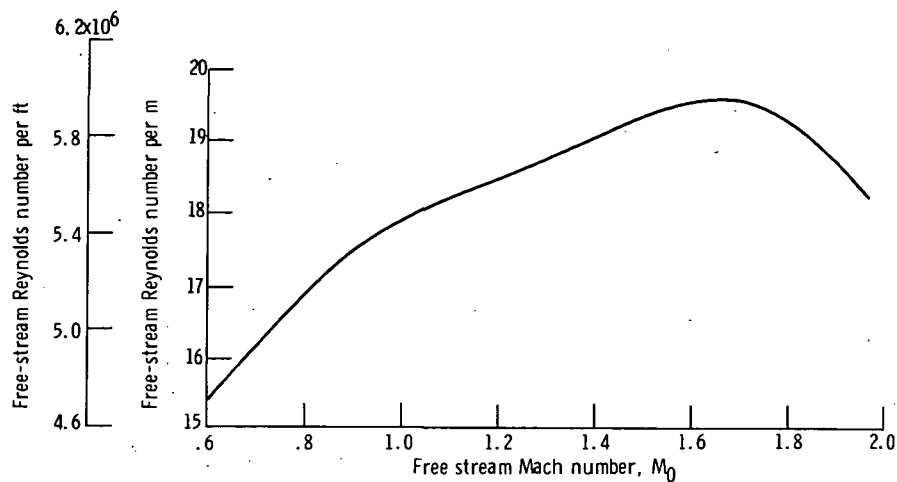


Figure 4. - Nominal-free-stream Reynolds number - Mach number profile.

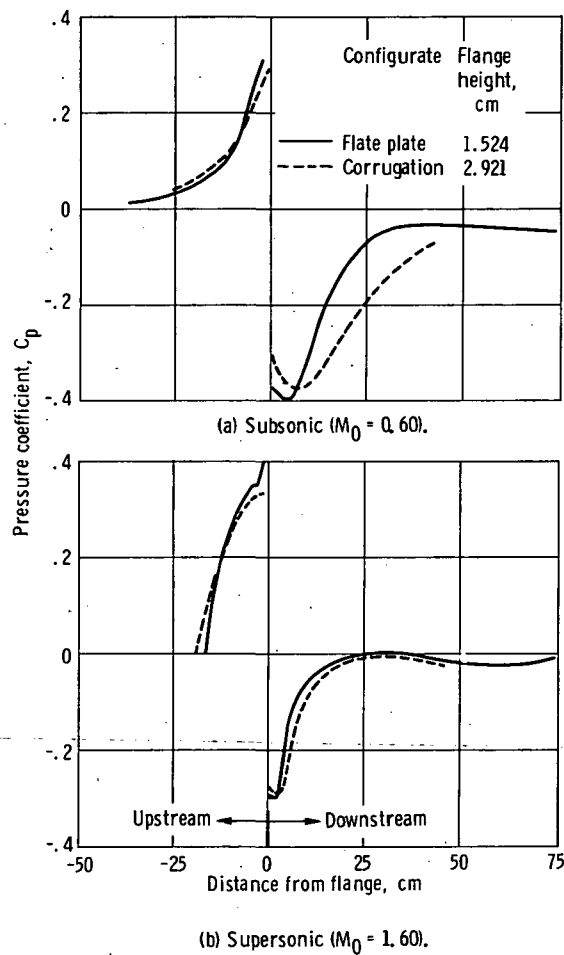


Figure 5. - Comparison of typical pressure coefficients upstream of leading edge and downstream of trailing edge of flange at subsonic and supersonic speeds with and without corrugations.

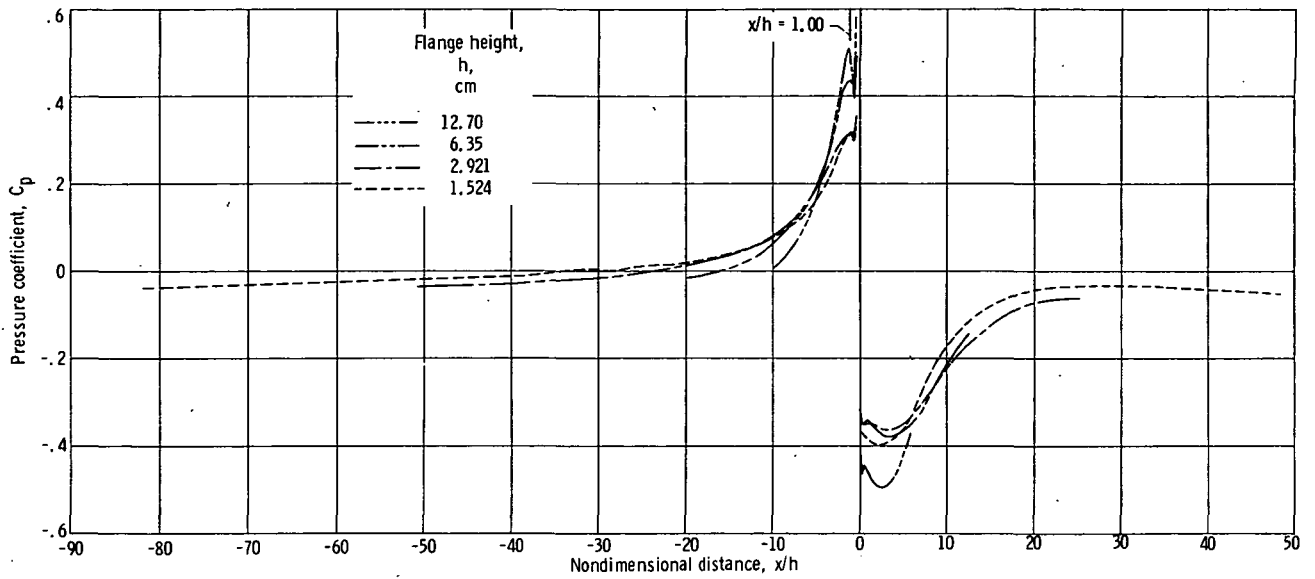


Figure 6. - Typical effect of flange height on flat plate peak and minimum pressure coefficient. Free-stream Mach number, 0.60.

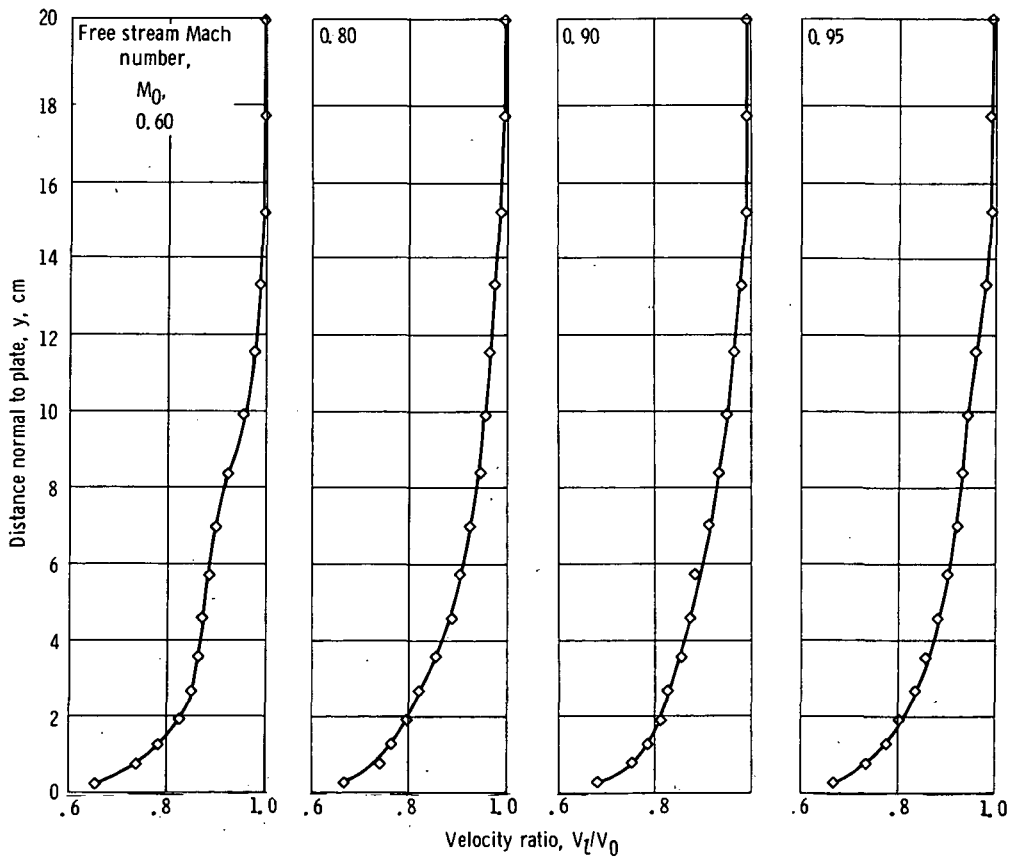


Figure 7. - Boundary-layer velocity profiles with flat plate and no flange.

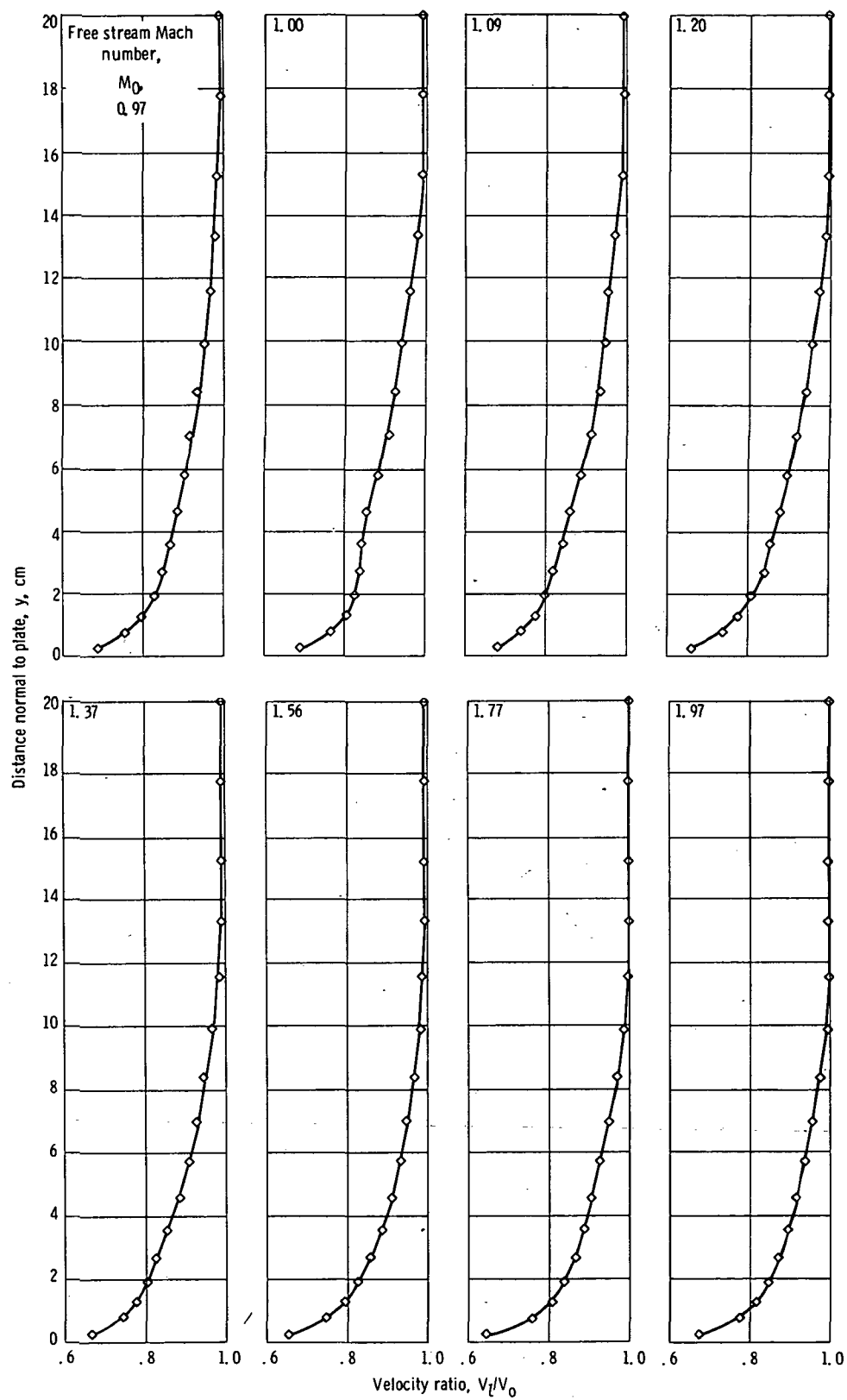


Figure 7. - Concluded.

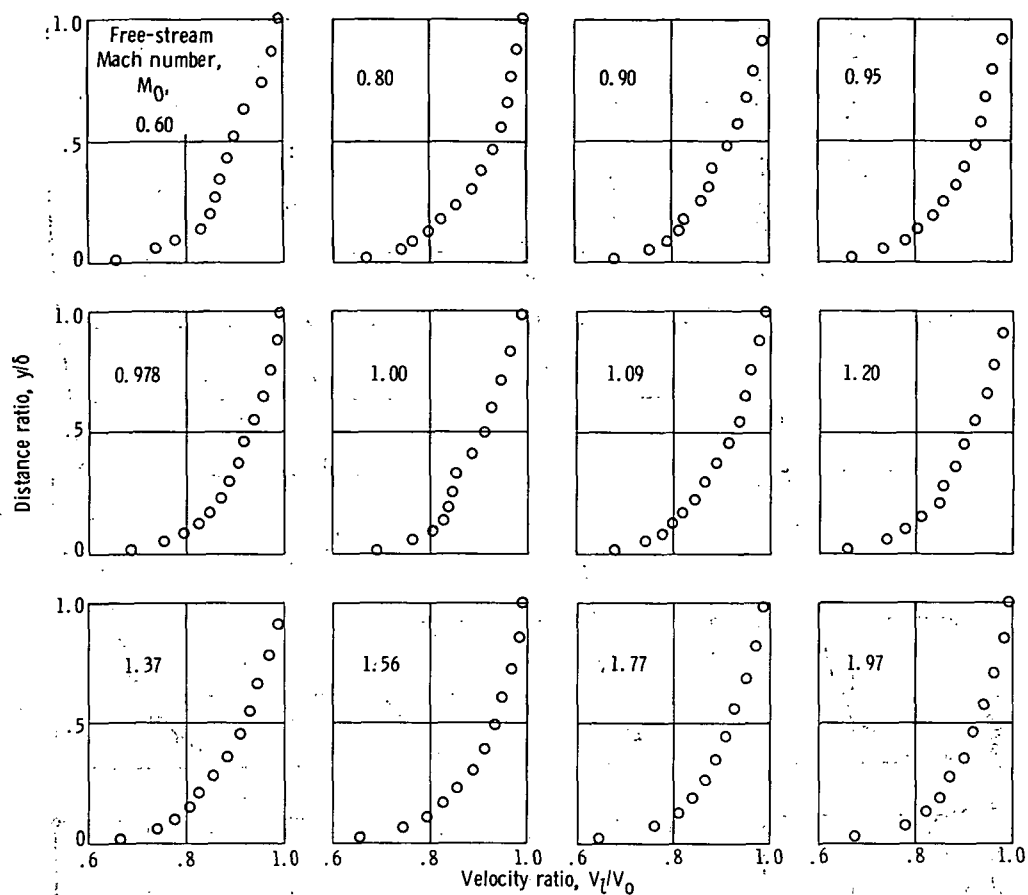


Figure 8. - Nondimensionalized boundary-layer profiles with flat plate and no flange.

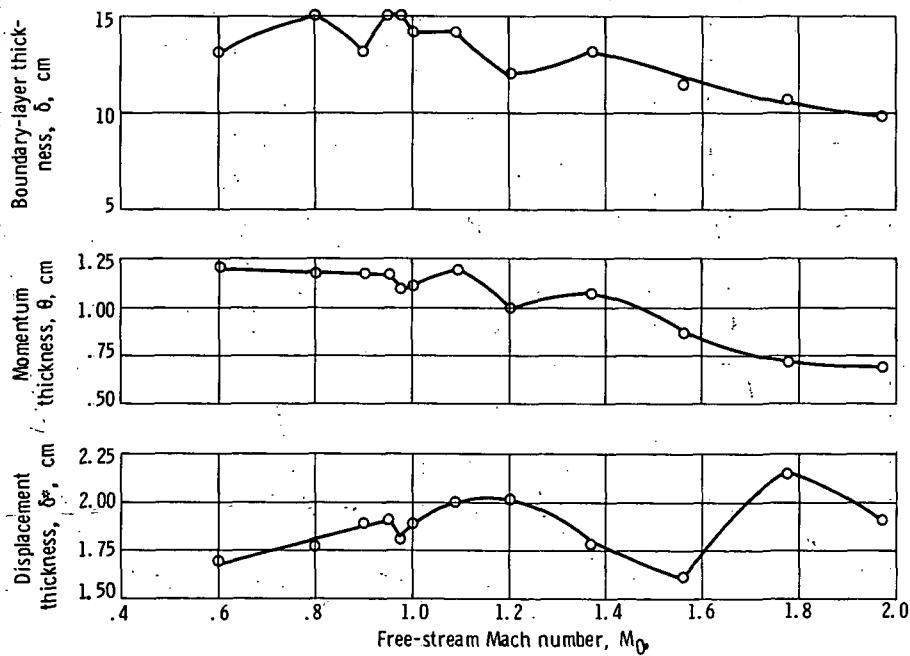
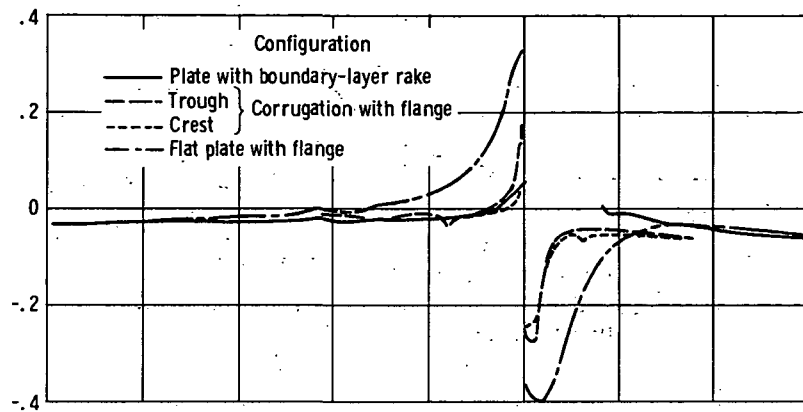
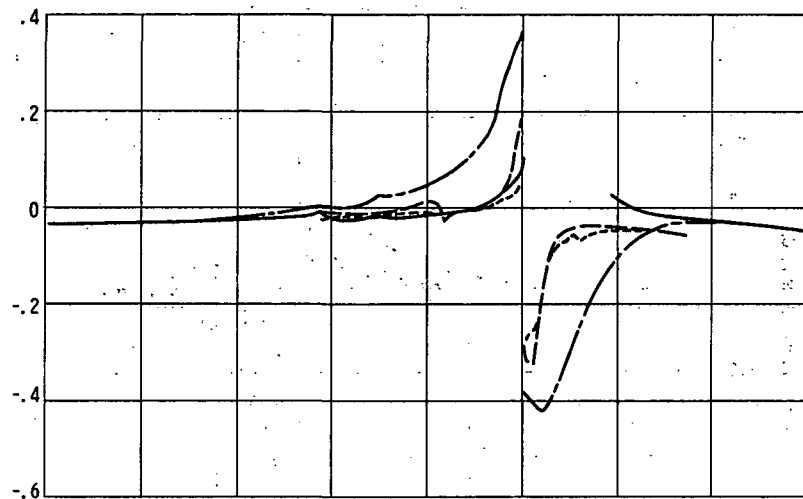


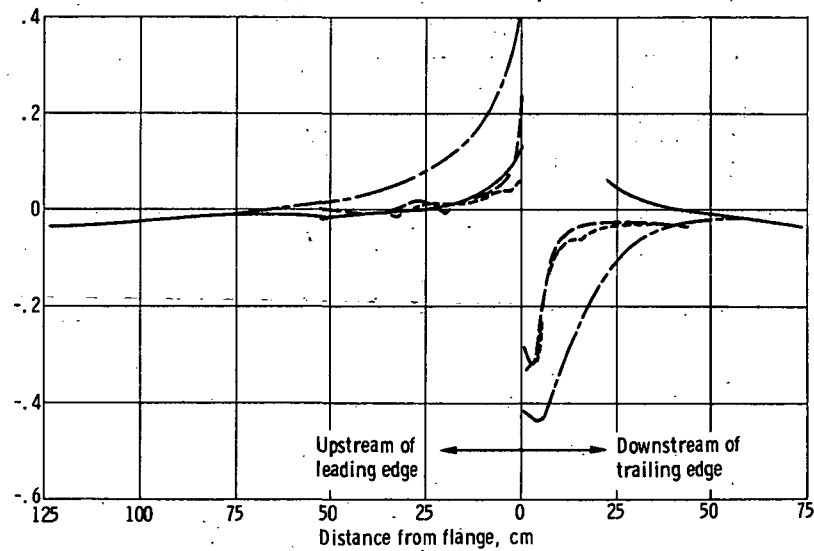
Figure 9. - Comparison of thickness parameters.



(a) Free-stream Mach number, 0.60

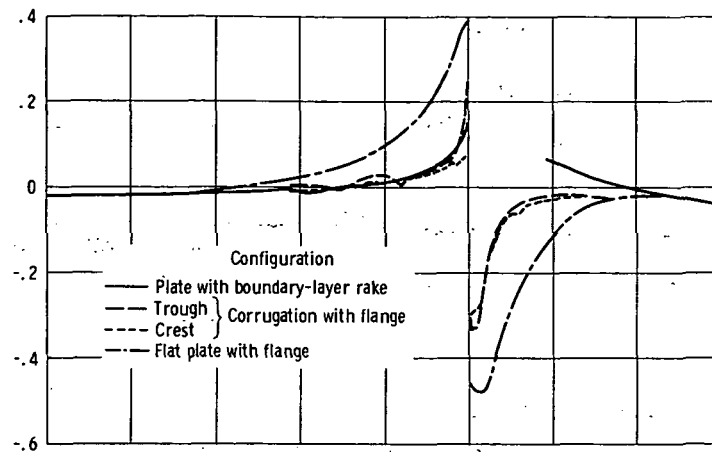


(b) Free-stream Mach number, 0.80

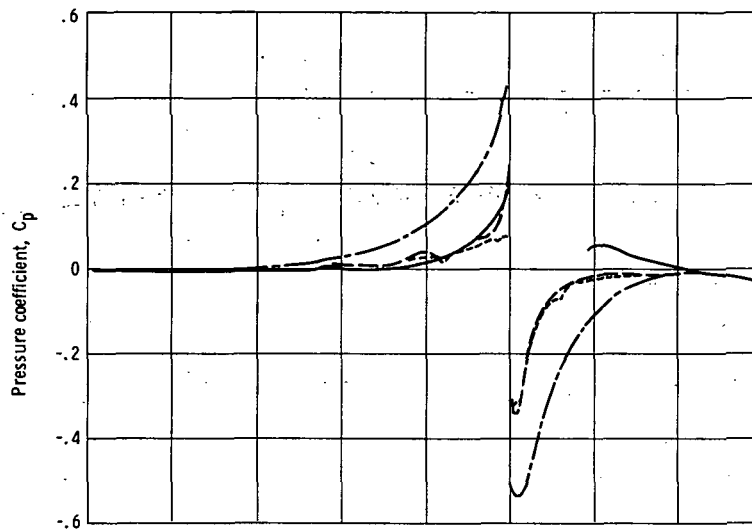


(c) Free-stream Mach number, 0.90

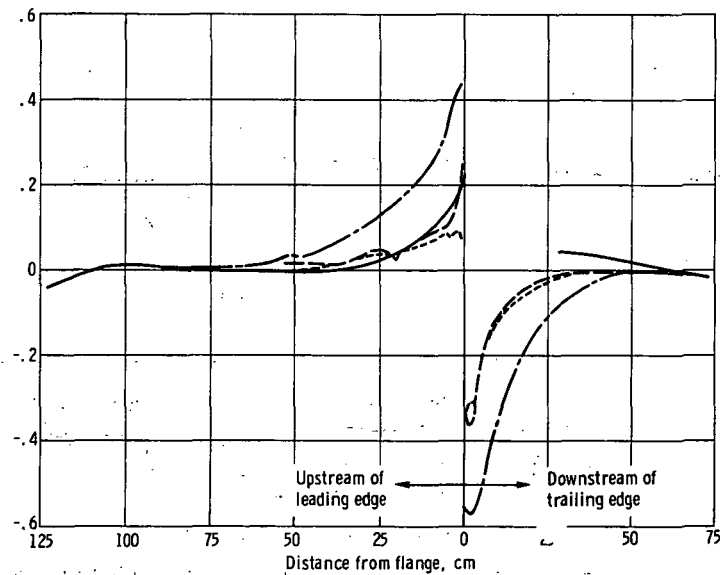
Figure 10. - Comparison of corrugated and flat-plate configurations with 1.524-centimeter flange on flat plate pressure coefficient.



(d) Free-stream Mach number, 0.95.

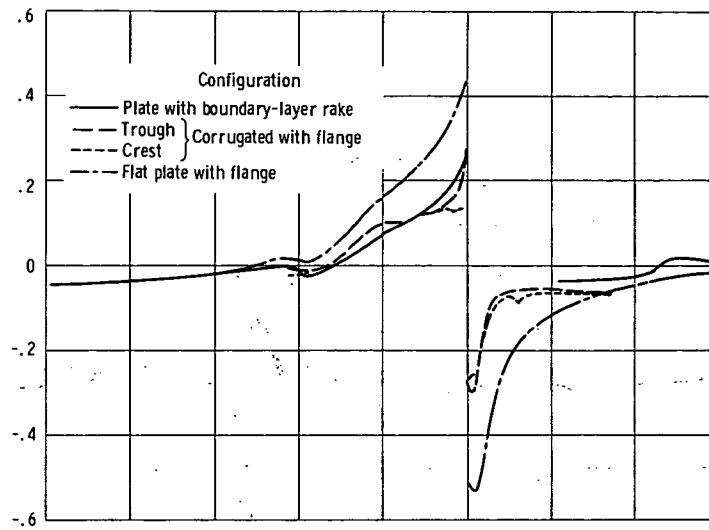


(e) Free-stream Mach number, 0.978.

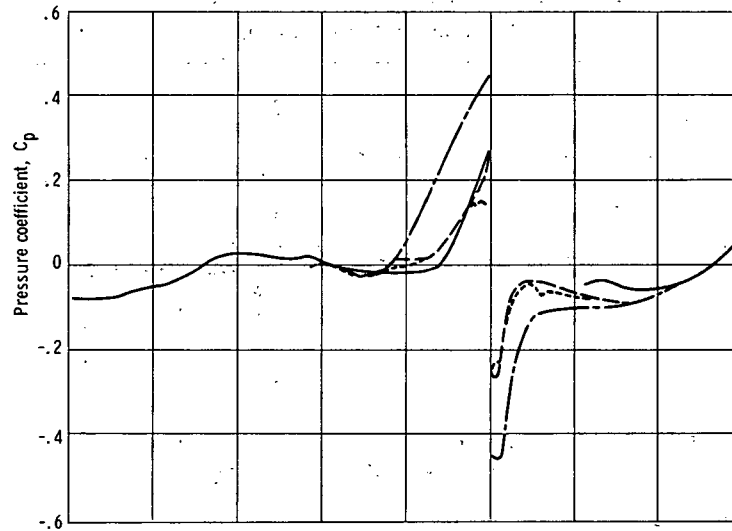


(f) Free-stream Mach number, 1.00.

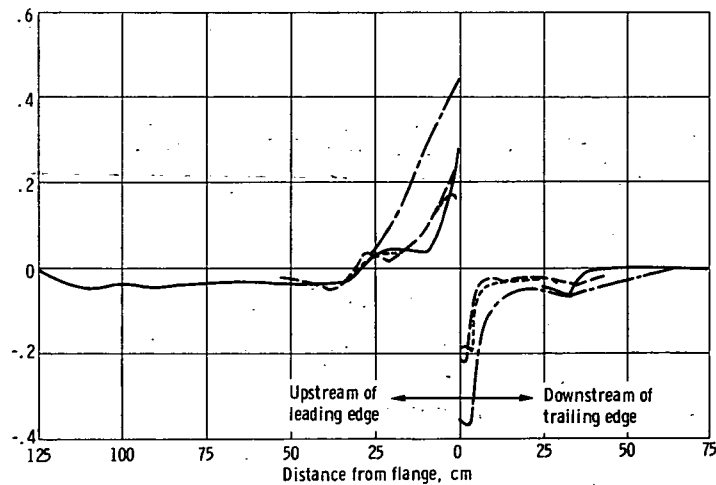
Figure 10. - Continued.



(g) Free-stream Mach number, 1.09.

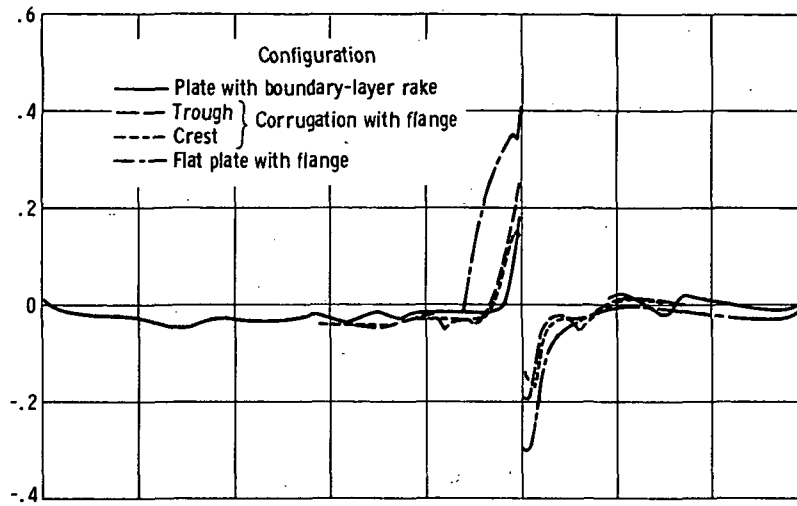


(h) Free-stream Mach number, 1.20.

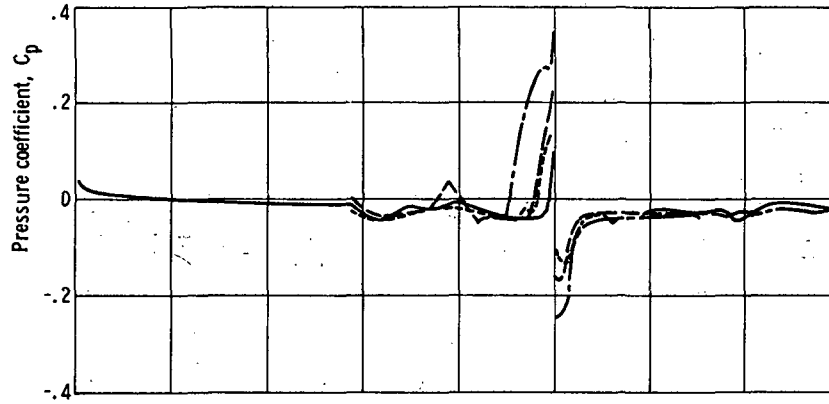


(i) Free-stream Mach number, 1.37.

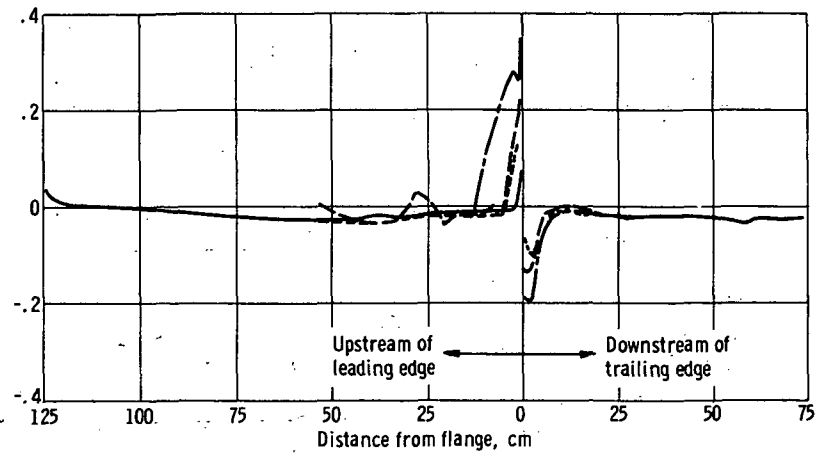
Figure 1Q - Continued



(j) Free-stream Mach number, 1.56.

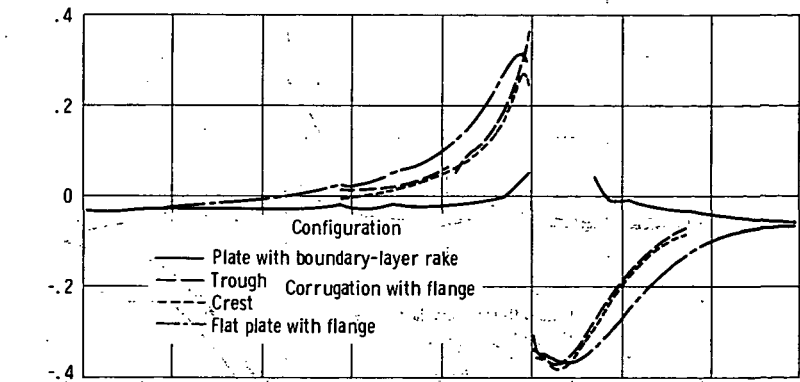


(k) Free-stream Mach number, 1.77.

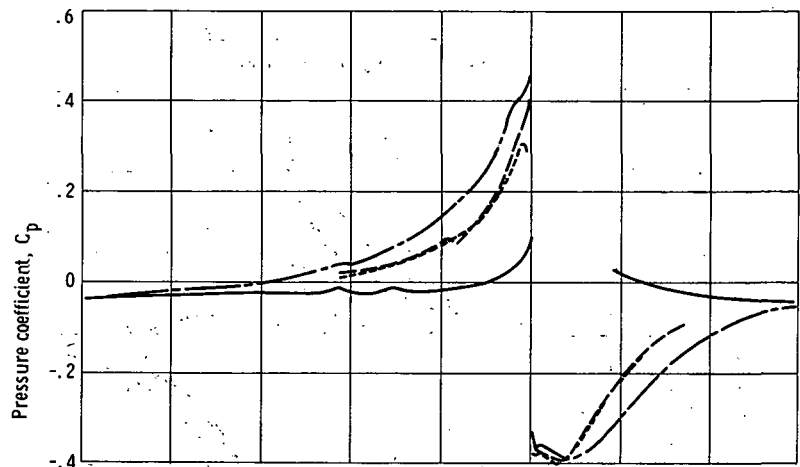


(l) Free-stream Mach number, 1.97.

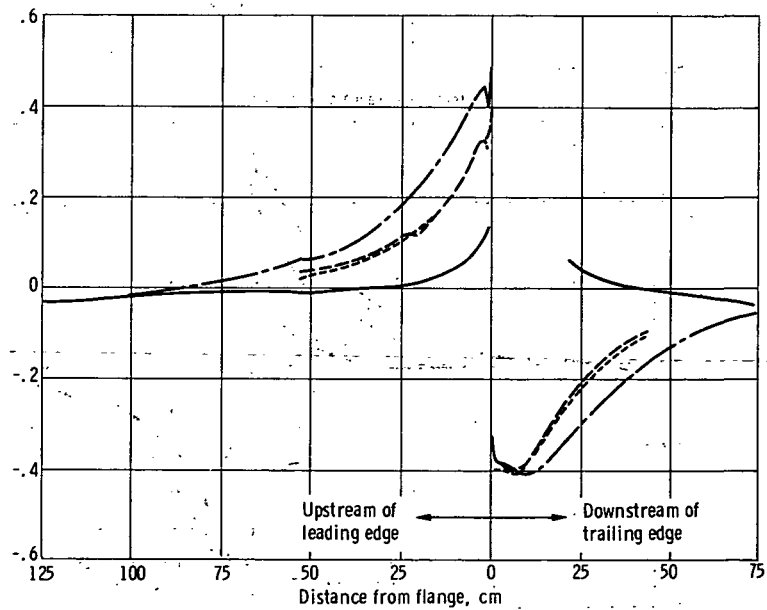
Figure 10 - Concluded



(a) Free-stream Mach number, $Q, 60$

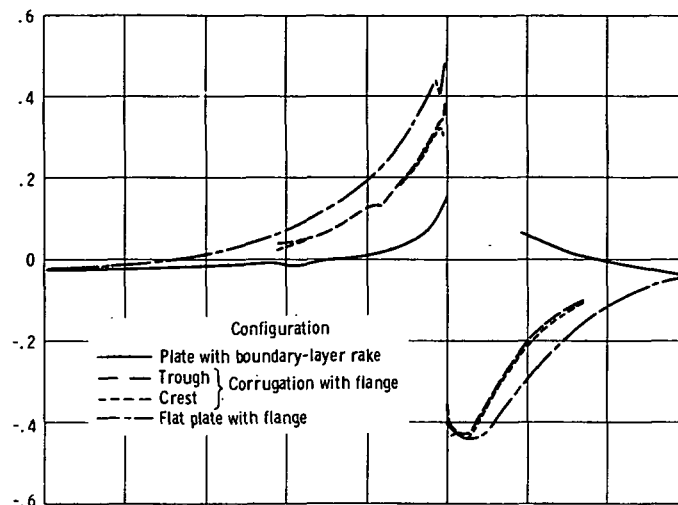


(b) Free-stream Mach number, $Q, 80$

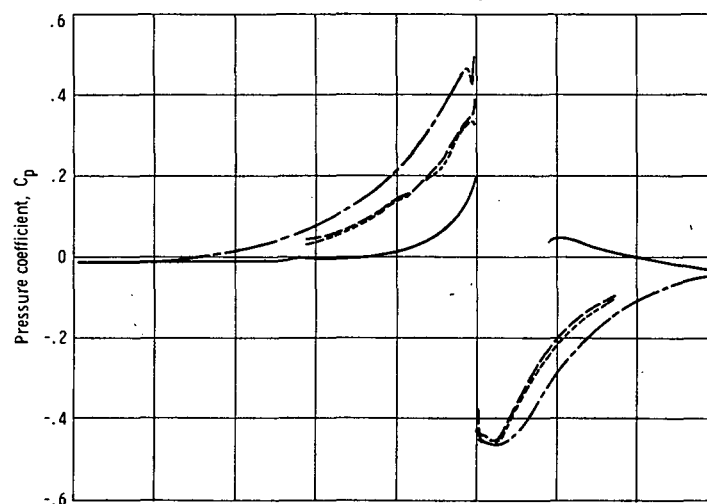


(c) Free-stream Mach number, $Q, 90$

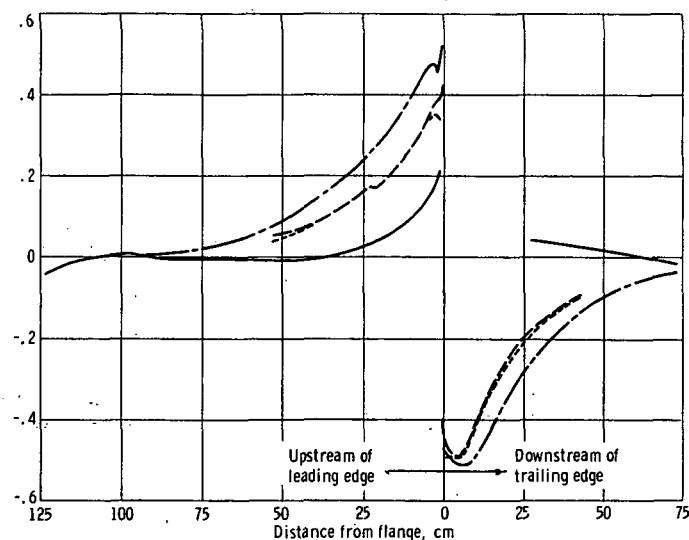
Figure 11. - Comparison of corrugated and flat-plate configurations with 2.921-centimeter flange on the flat plate pressure coefficient.



(d) Free-stream Mach number, $Q 95$.

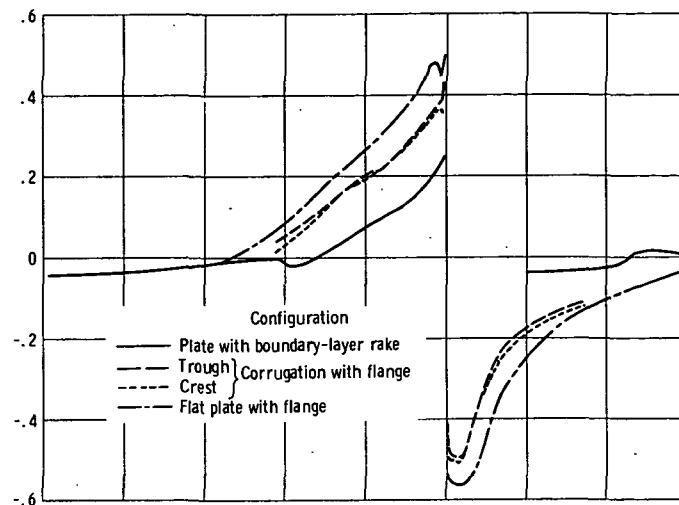


(e) Free-stream Mach number, $Q 97.8$.

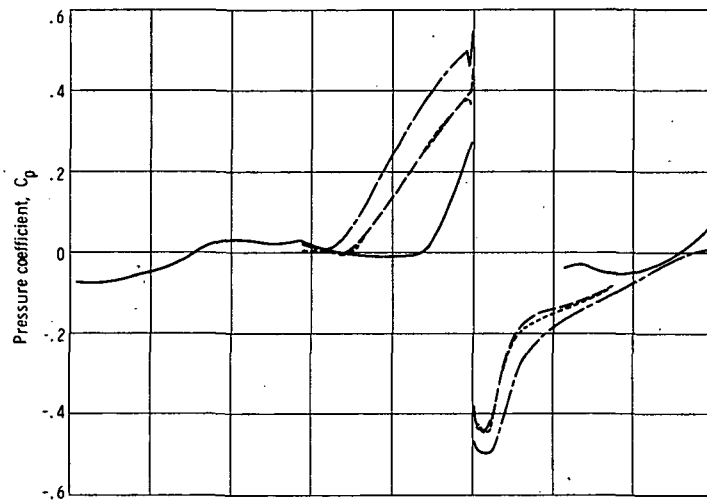


(f) Free-stream Mach number, $Q 1.00$.

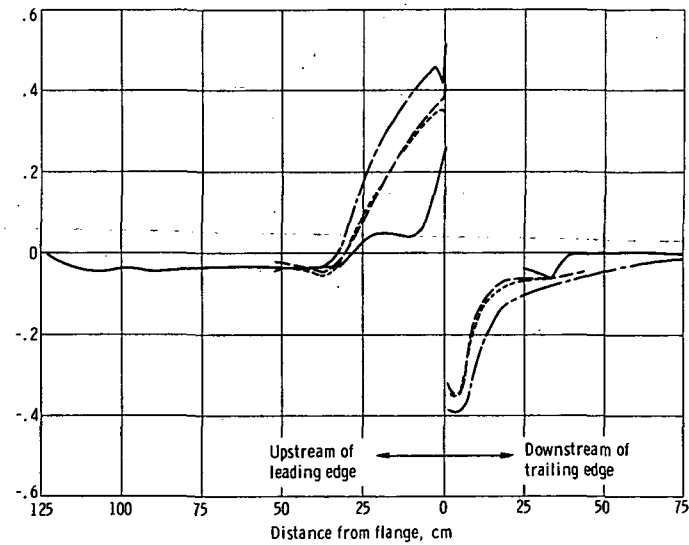
Figure 11.. - Continued.



(g) Free-stream Mach number, 1.09.



(h) Free-stream Mach number, 1.20.



(i) Free-stream Mach number, 1.37.

Figure 11. - Continued.

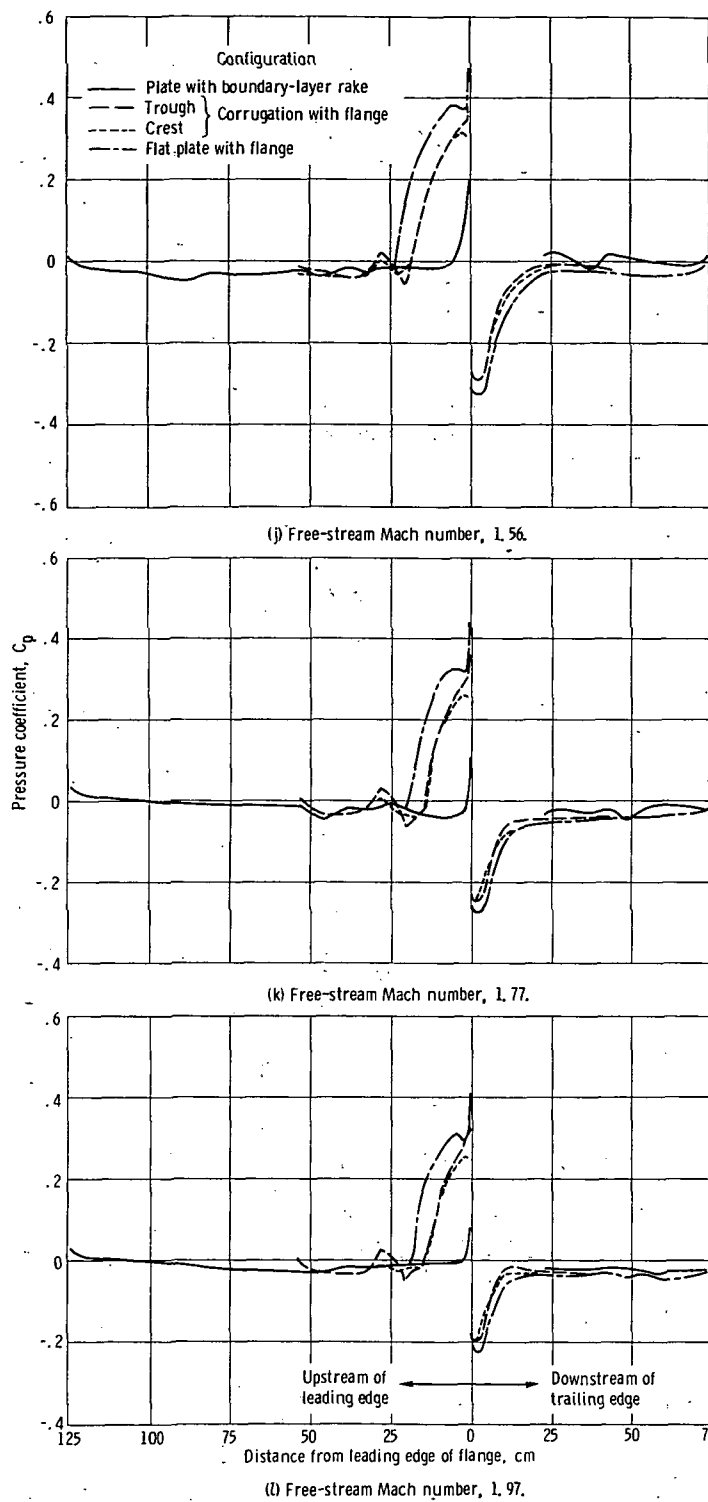


Figure 11. - Concluded.

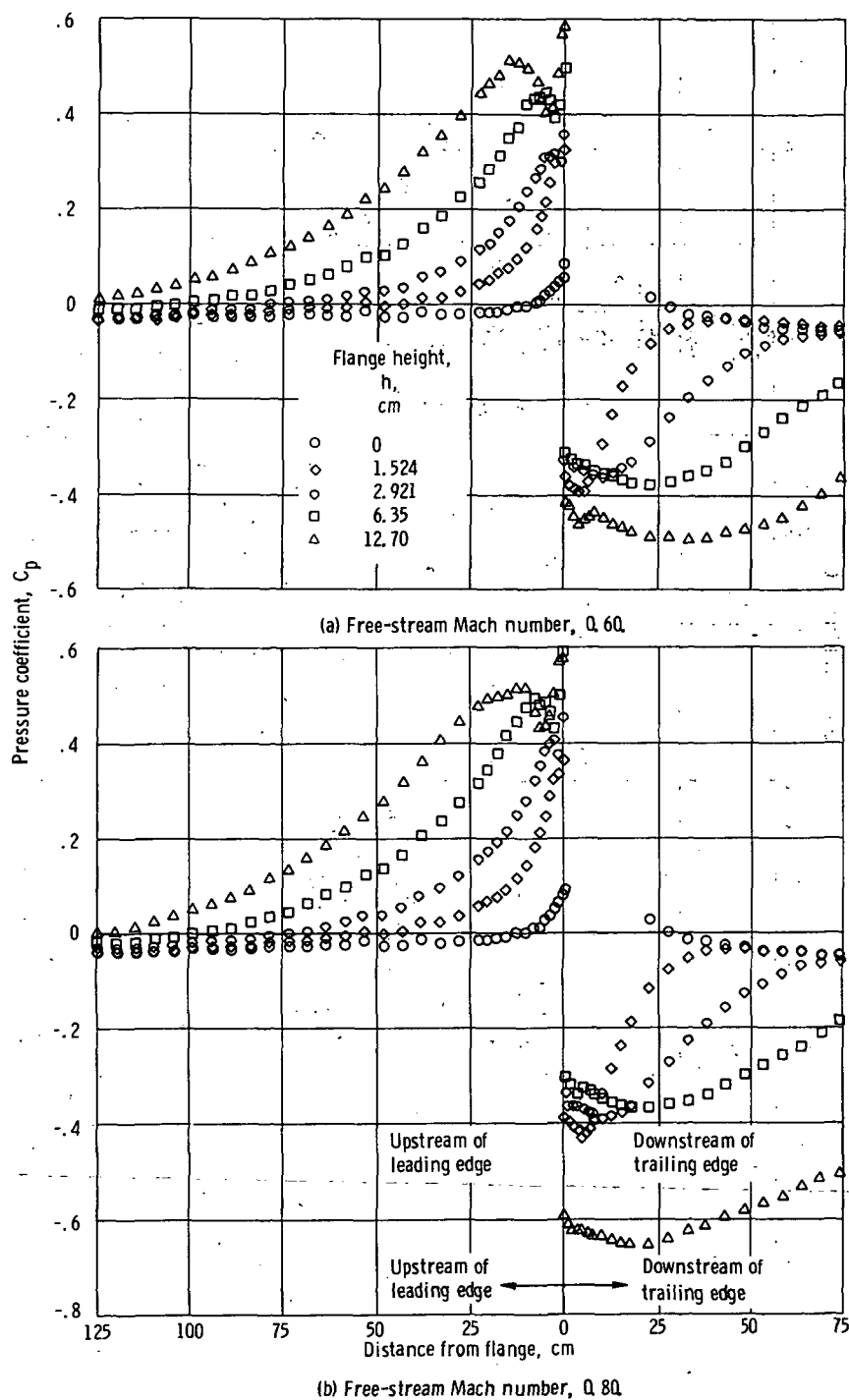
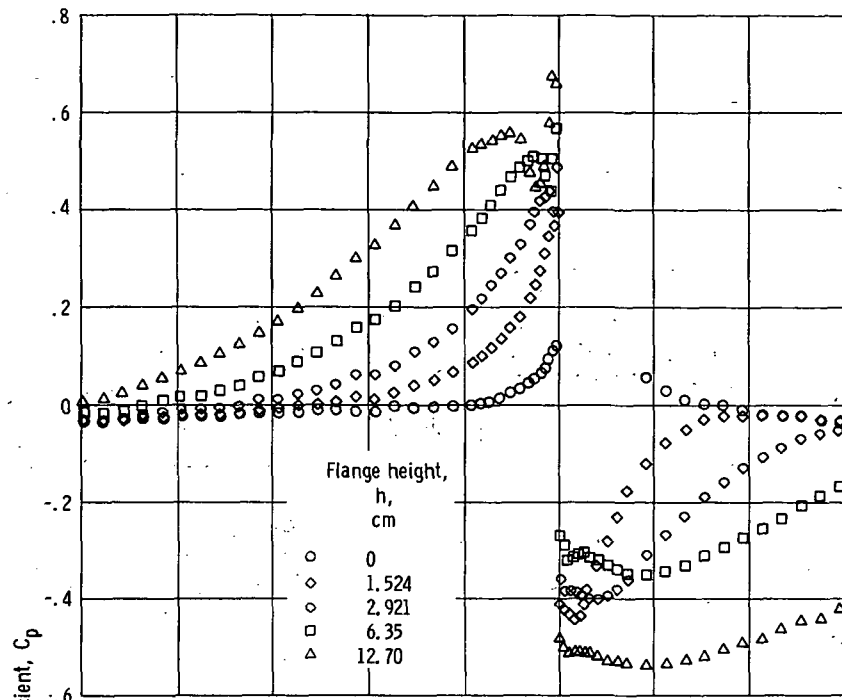
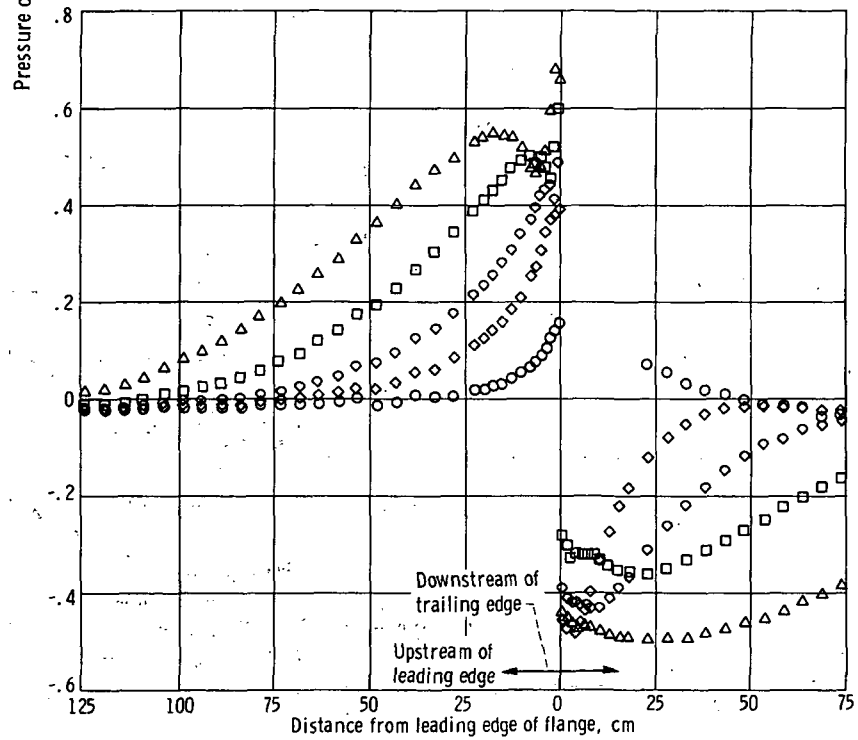


Figure 12. - Effect of flange height on flat plate pressure coefficient upstream and downstream of flange. Flange width, 1.571 centimeter.

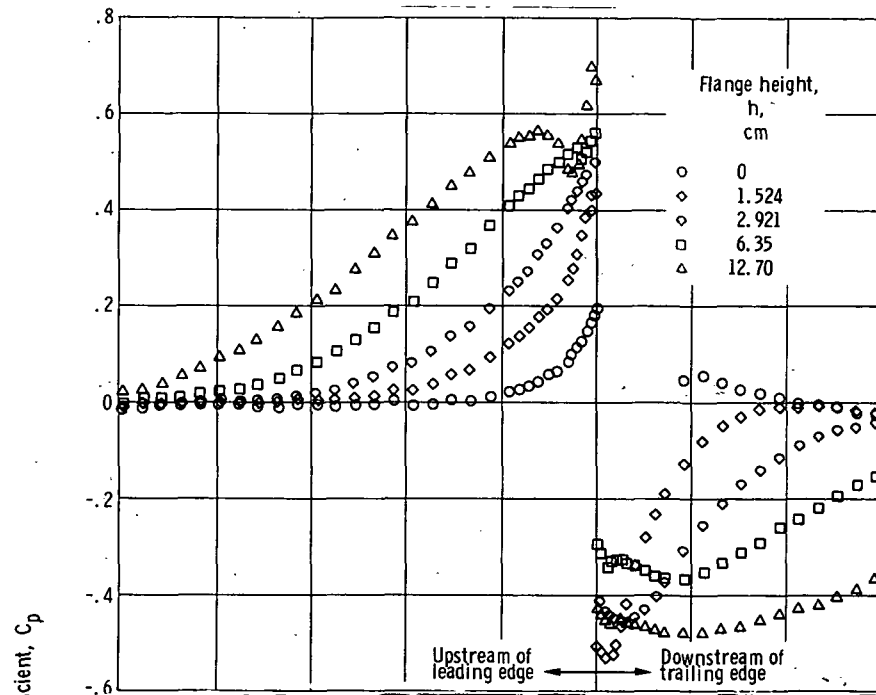


(c) Free-stream Mach number, 0.90.

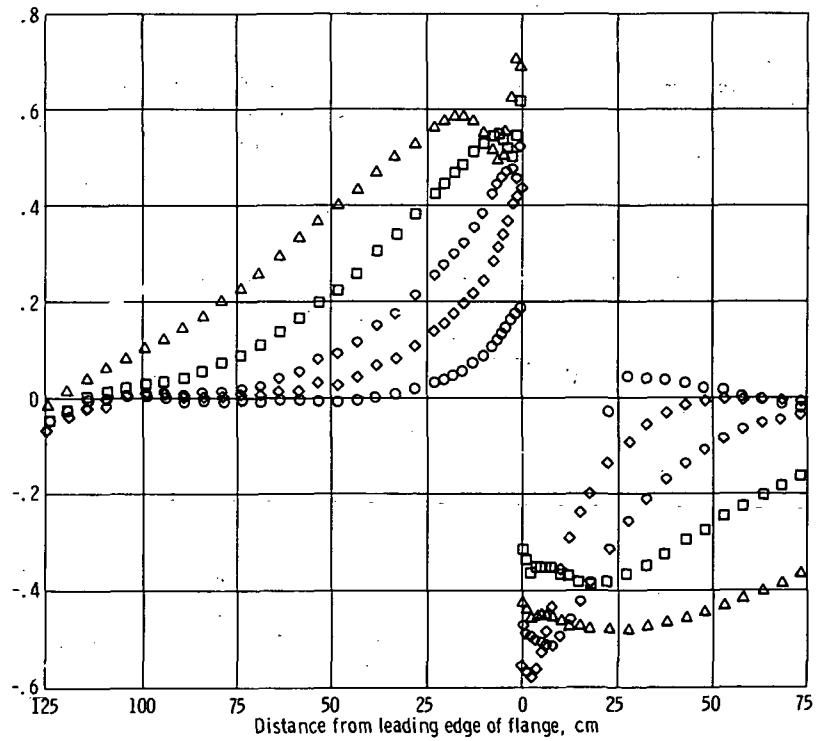


(d) Free-stream Mach number, 0.95.

Figure 12. - Continued.

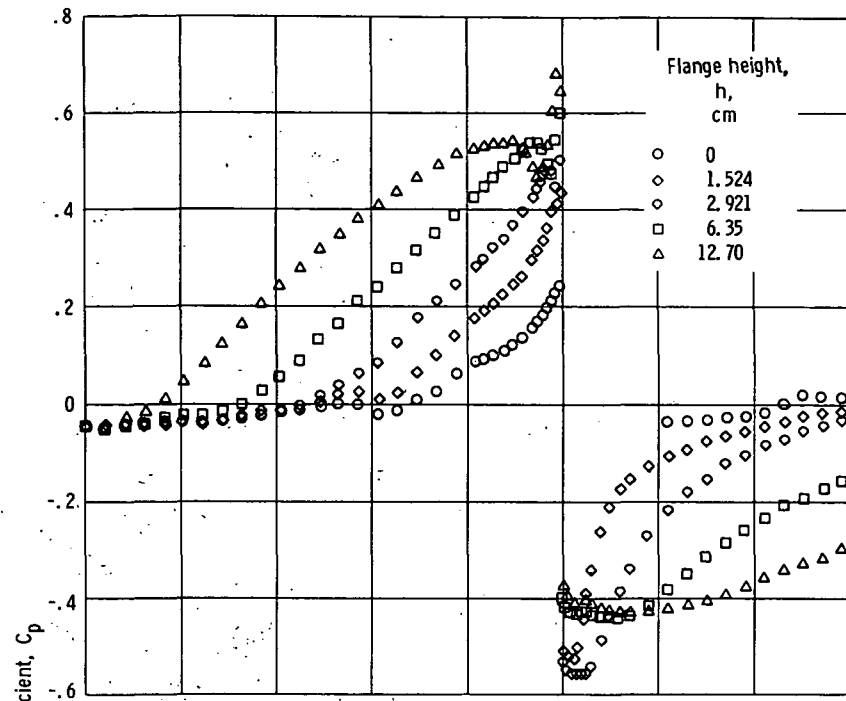


(e) Free-stream Mach number, 0.978.

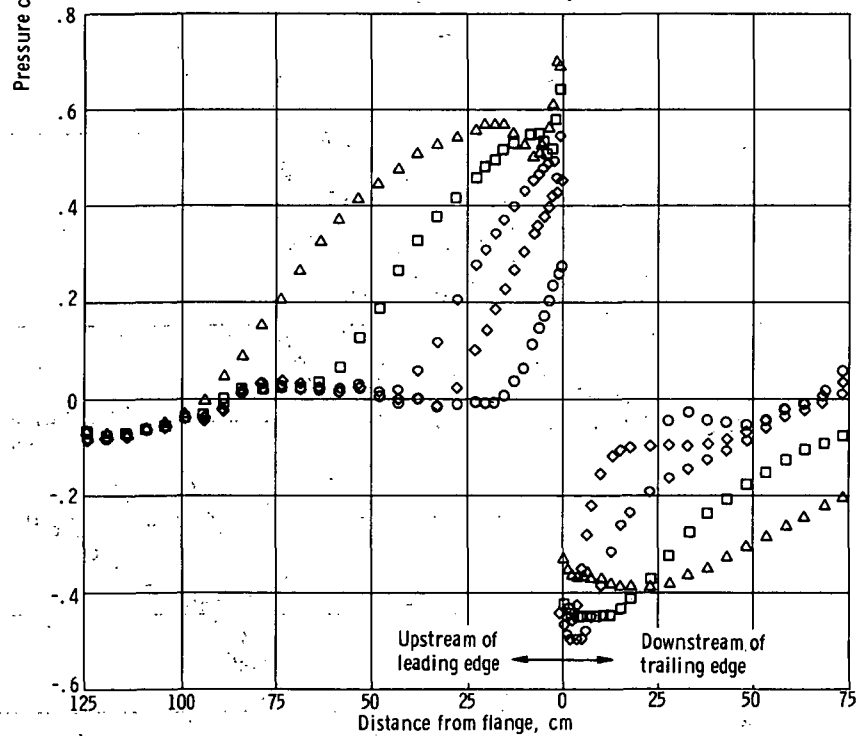


(f) Free-stream Mach number, 1.00.

Figure 12. - Continued.

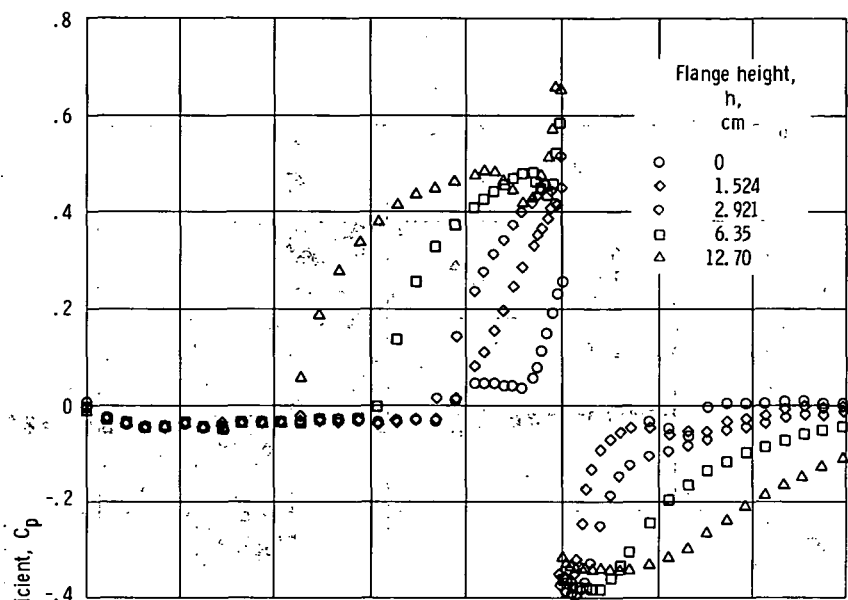


(g) Free-stream Mach number, 1.09.

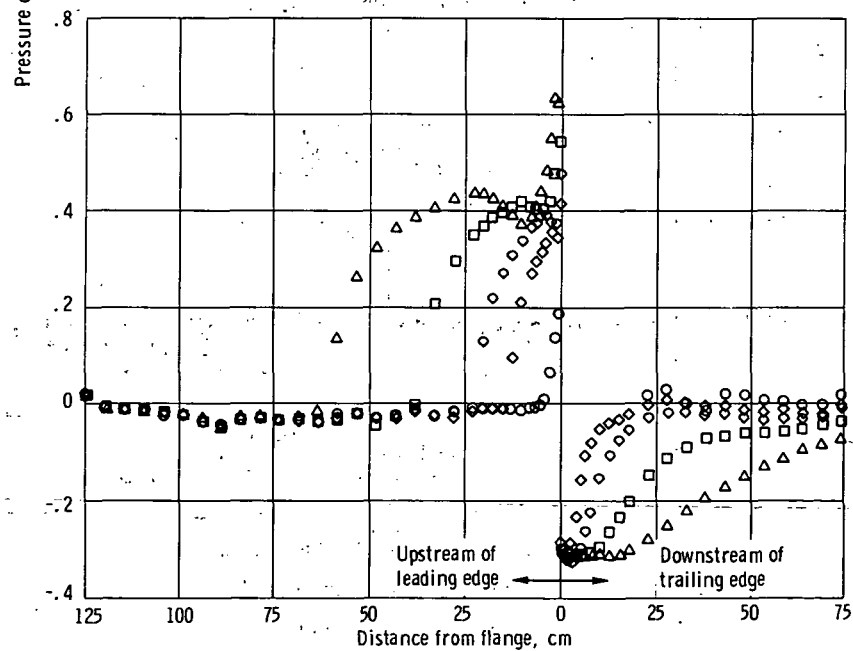


(h) Free-stream Mach number, 1.20.

Figure 12. - Continued.

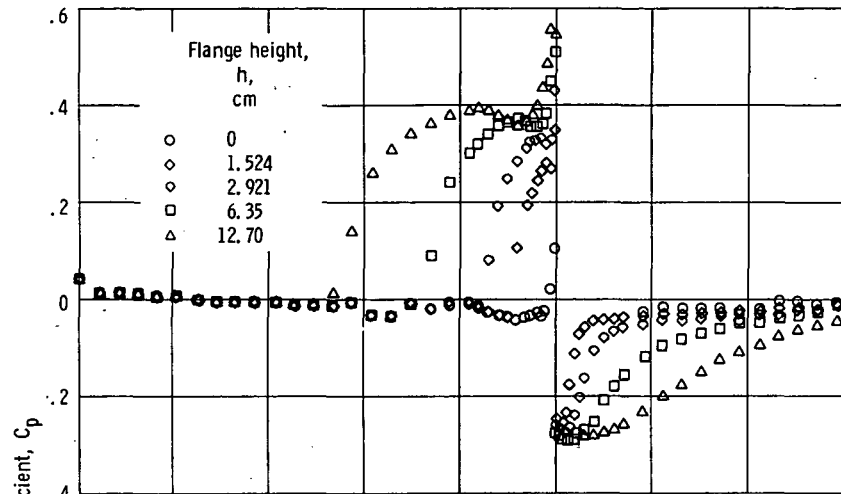


(i) Free-stream Mach number, 1.37.

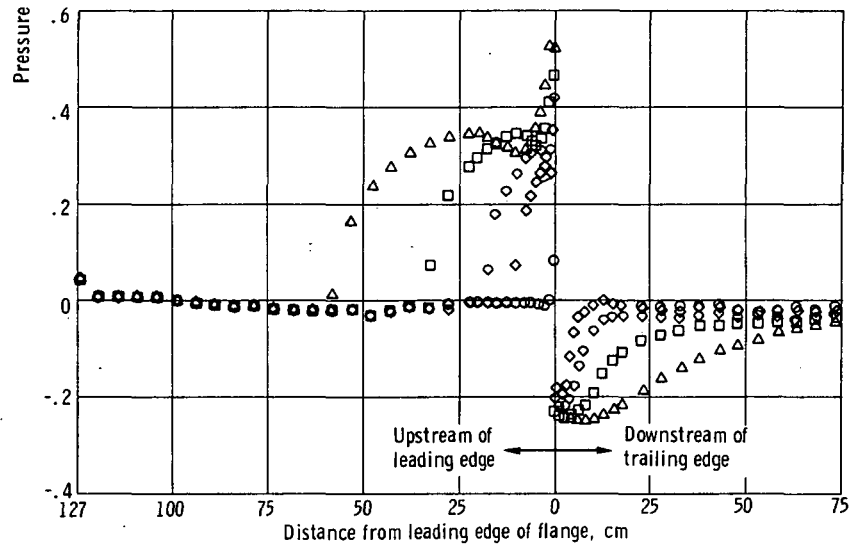


(j) Free-stream Mach number, 1.56.

Figure 12. - Continued.



(k) Free-stream Mach number, 1.77.



(l) Free-stream Mach number, 1.97.

Figure 12. - Concluded.



POSTMASTER : If Undeliverable (Section 158
Postal Manual) Do Not Return

"The aeronautical and space activities of the United States shall be conducted so as to contribute . . . to the expansion of human knowledge of phenomena in the atmosphere and space. The Administration shall provide for the widest practicable and appropriate dissemination of information concerning its activities and the results thereof."

—NATIONAL AERONAUTICS AND SPACE ACT OF 1958

NASA SCIENTIFIC AND TECHNICAL PUBLICATIONS

TECHNICAL REPORTS: Scientific and technical information considered important, complete, and a lasting contribution to existing knowledge.

TECHNICAL NOTES: Information less broad in scope but nevertheless of importance as a contribution to existing knowledge.

TECHNICAL MEMORANDUMS: Information receiving limited distribution because of preliminary data, security classification, or other reasons. Also includes conference proceedings with either limited or unlimited distribution.

CONTRACTOR REPORTS: Scientific and technical information generated under a NASA contract or grant and considered an important contribution to existing knowledge.

TECHNICAL TRANSLATIONS: Information published in a foreign language considered to merit NASA distribution in English.

SPECIAL PUBLICATIONS: Information derived from or of value to NASA activities. Publications include final reports of major projects, monographs, data compilations, handbooks, sourcebooks, and special bibliographies.

TECHNOLOGY UTILIZATION PUBLICATIONS: Information on technology used by NASA that may be of particular interest in commercial and other non-aerospace applications. Publications include Tech Briefs, Technology Utilization Reports and Technology Surveys.

Details on the availability of these publications may be obtained from:

SCIENTIFIC AND TECHNICAL INFORMATION OFFICE

NATIONAL AERONAUTICS AND SPACE ADMINISTRATION
Washington, D.C. 20546